Turning to the dark side: Evolutionary history and molecular species delimitation of a troglomorphic lineage of armoured harvestman (Opiliones: Stygnopsidae)

Jesús A. Cruz-López *,[1,2], Rodrigo Monjaraz-Ruedas[1,2] & Oscar F. Francke[2]

[1] Posgrado en Ciencias Biológicas, Universidad Nacional Autónoma de México, Av. Universidad 3000, C.P. 04510, Coyoacán, Mexico City, Mexico; Jesús A. Cruz-López [thelyphonidito@gmail.com] — [2] Colección Nacional de Arácnidos, Departamento de Zoología, Instituto de Biología, Universidad Nacional Autónoma de México. 3er circuito exterior s/n. Apartado postal 70-153. C.P. 04510, Ciudad Universitaria, Coyoacán, Mexico City, Mexico — * Corresponding author

Abstract. From a biological point of view, caves are one of the most exciting environments on Earth, considered as evolutionary laboratories due to the adaptive traits (troglomorphisms) usually exhibited by the fauna that inhabit them. Among Opiliones, the family Stygnopsidae contains cave-inhabiting members who exhibit some degree of troglomorphic characters, such as *Minisge* gen.n., a lineage formed by two new troglomorphic species from the Huautla Cave System, Oaxaca, Mexico, one of the deepest and most complex cave systems in the World. One of the new species inhabits the middle depths (~ 400 to ~ 600 m), whereas the other one is considerably shallower (~ 20 to ~ 200 m). Using the barcoding gene (CO1), we tested the morphology-based species delimitation hypothesis using genetic distances, likelihood-based and bayesian-based methods (ABGD, GMYC and bPTP), which give different results with respect to morphology. The shallower species exhibits considerable gene flow among the various caves sampled and the genetic data support our morphology-based conclusions; whereas the deeper species shows less gene flow among some of the caves in the system, and the genetic data contradict our morphology-based conclusion that there is only one species involved. However, the genetic differences among the populations sampled vary primarily in the third codon position and represent synonymous mutations. Finally, the two species of *Minisge* gen.n. probably diverged 3.9 Mya according to a time-calibrated phylogeny, but at this time it is not possible to determine when they colonized the cave environment, although we favour the hypothesis that each species of *Minisge* colonized the caves independently: the deeper inhabitant, which exhibits a greater degree of troglomorphisms, first; and subsequently the shallower inhabitant, which exhibits a lesser degree of troglomorphisms.

Key words. Species delimitation, new genus, haplotype network, divergence time, colonization.

1. Introduction

Caves are one of the most adverse environments on Earth, as the restricted access to food and the extreme conditions of darkness and humidity make these habitats very challenging for living organisms (Hüppop 2012). Despite this, many taxa have colonized these subterranean environments, including arthropods and vertebrates (Howart & Hoch 2012; Culver 2016). Some of these animals have become fully established in cave systems, so they have evolved specific morphological adaptations (= troglomorphisms) such as cuticular depigmentation, elongation of appendages and reduction or loss of eyes (Trajano & Cobolli 2012). Troglobitic animals (those who exhibit troglomorphisms) are excellent models for studies of the evolution of those adaptations and for studies of morphological convergence among distant lineages (Culver et al. 1995; Sbordoni et al. 2000; Jeffery 2005; Cruz-López et al. 2016).

In the class Arachnida, troglobites are known for 9 of the 11 extant orders; only Thelyphonida and Solifugae are without representatives (Ribera 2004). One of the orders with many troglobitic taxa is Opiliones (Reddell 2012). Within this order, there are families with some taxa partly or completely associated with caves or hypogean habitats, like Ischyropsalididae, Paranonychi-
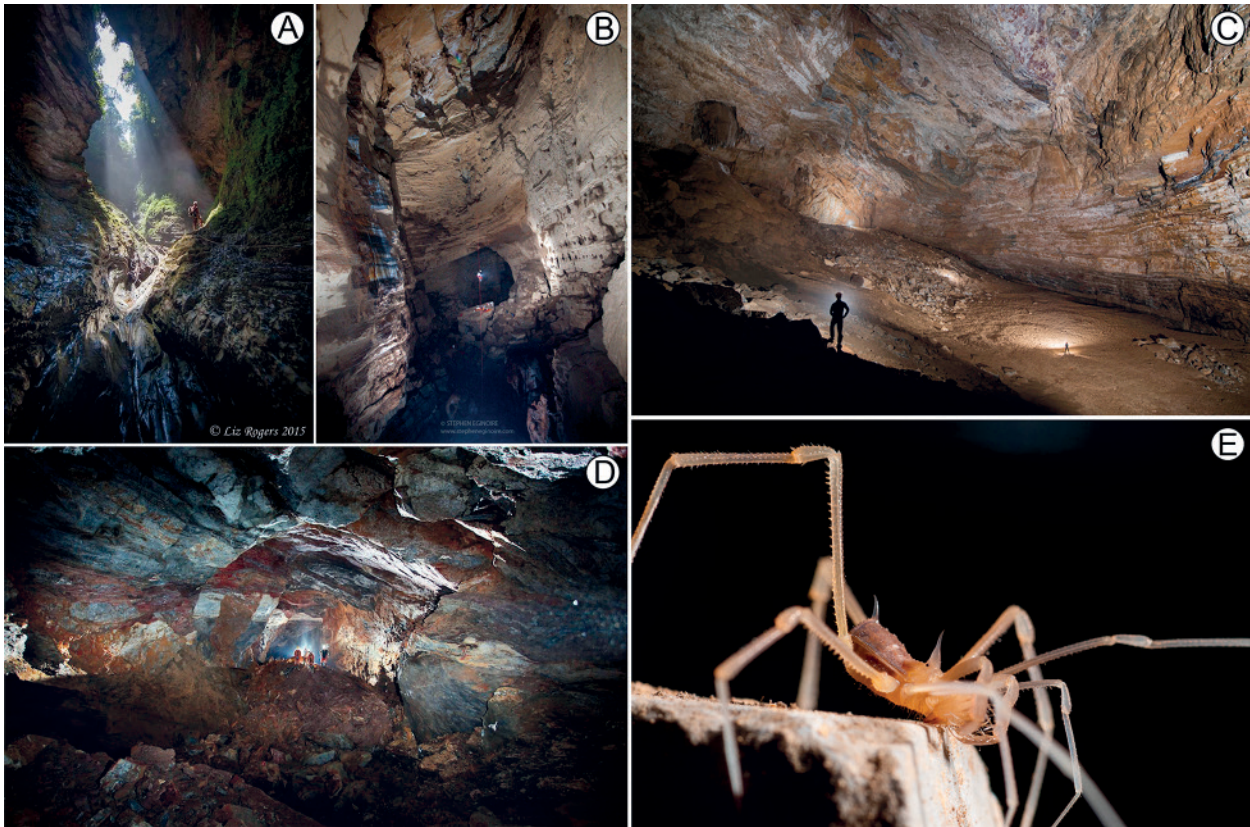
Fig. 1. Huautla Cave System: (**A** – **D**) views of different areas into Huautla cave system; (**E**) live specimen of *Minisge sagai* sp.n. Photos by (A) Liz Rogers, (B) Stephen Eginoire, (C) Chris Higgins, (D) and (E) Jean Krejka.

dae, Phalangodidae and Stygnopsidae (DERKARABETIAN et al. 2010; HEDIN & THOMAS 2010; SCHÖNHOFER et al. 2015; CRUZ-LÓPEZ & FRANCKE 2017). Convergent evolution in troglomorphic morphology has been confirmed among different lineages, at least in the North American phalangodids and sclerobunines (Paranonychidae) and the European *Ischyropsalis* C.L. Koch, 1839 (DERKARABETIAN et al. 2010; HEDIN & THOMAS 2010; SCHÖNHOFER et al. 2015). It is remarkable that troglomorphic species in those studies have a limited distribution range, generally restricted to a single cave or the nearest caves of the same system (DERKARABETIAN & HEDIN 2014). However, only in the North American travunioids, divergent troglomorphic lineages have been associated with the climatic fluctuations during the Pleistocene, wherein drier/warmer periods could drive these species to seek refuge from climate extremes in the underground habitats, and subsequent cave colonization and morphological adaptation (DERKARABETIAN et al. 2010).

In Stygnopsidae, at least 10 genera and 23 species have been found associated with cave systems and some of them exhibit different degrees of modification in the troglomorphic characters (CRUZ-LÓPEZ & FRANCKE 2017). According to the phylogenetic framework hypothesis of the family proposed by CRUZ-LÓPEZ & FRANCKE (2017), troglobitic species have evolved convergently with similar morphologies, such as *Troglostygnopsis* Šilhavý, 1974 and *Mictlana* Cruz-López & Francke, 2015 (CRUZ-LÓPEZ & FRANCKE 2015, 2017) which were formerly considered to belong to the same lineage; unfortunately, time calibrated phylogenies for these groups have not been made.

Although several taxonomic studies on Stygnopsidae were published in recent years, a considerable number of undescribed troglomorphic taxa, mostly from Mexico, await to be studied. This is the case of the taxa treated here: a new genus, *Minisge* gen.n., with two new and sympatric troglomorphic species, both endemic to the Huautla Cave System in Oaxaca, Mexico. This cave system is remarkable because of its depth and extension; to date explorers have reached a depth of ~1,500 m from the entrance, and the system has over 20 entrances connected at great depth, with the entire system extending over 65 km (Figs. 1 & 11) (STEELE & SMITH 2012). It is significant that the two new species described here are sister species and are sympatric, generally found in the same caves but at different depths and in different microhabitats (not syntopic) and it is the first such case reported in Laniatores. Therefore, using the ribosomal barcoding cytochrome *c* oxidase sub-unit I (COI) gene fragment, we investigated the relationships and evaluated species limits, as well as the gene flow within the species throughout the cave system. Additionally, we estimated the diversification times for the genus. Finally, we discuss the importance of cave environments as speciation forces in troglomorphic species.

2. Material and methods

We conducted three explorations to the Cave System of Huautla de Jiménez, Oaxaca, Mexico (Fig. 1). These field trips took place every April from 2014 to 2016, because cave exploration is viable during the dry season, when the watercourses are low and access to deepest areas is easiest and least dangerous. Cave exploration was possible with assistance provided by the Proyecto Espeleológico Sistema Huautla (PESH project), which is a team of speleologists who have investigated this system for decades. During the fieldwork, we collected many samples of troglomorphic arachnids and preserved them in 96% ethanol, including the main taxa treated here. Despite extensive searching and collecting for arachnids on the surface in the Huautla region, we have found no close epigean relatives of the two new species described here, although two members of the same subfamily are present: *Hoplobunus* Banks, 1900 and *Isaeus* Sørensen, 1932.

2.1. Taxonomic methods

In the laboratory we labelled and catalogued the specimens collected during the fieldtrips and the type material is deposited at Colección Nacional de Arácnidos (CNAN) in the Universidad Nacional Autónoma de México (UNAM). The specimens were studied under a Nikon SMZ 625 stereomicroscope. Color photographs were taken with Nikon Coolpix S10 camera attached to the microscope. Electronic microphotographs were taken in a Hitachi SU1510 SEM at Instituto de Biología, in the UNAM, as part of the Laboratorio Nacional de Biodiversidad (LaNaBio network). For the microphotograph samples (SEM), we followed the procedure proposed by Acosta et al. (2007). Terminologies of external morphology, scutum shape, pedipalpal armature, and male genitalia follow Cruz-López & Francke (2015, 2017), Acosta et al. (2007), Kury & Medrano (2016) and Kury & Villarreal (2015), respectively. Photographs were edited using Photoshop CS5; figures of the phylogenetic trees were edited using FIGTREE v. 1.3.1 and Adobe Illustrator v. CC.

2.2. Molecular methods

For DNA extraction, one of the third pair of legs of each specimen was dissected and preserved in 96% ethanol. Genomic DNA extraction was made using DNeasy tissue kit (Qiagen®) following supplier procedures. The COI gene was amplified using the pair of primers LCO1490 and HCO2198 (Folmer et al. 1994). PCR reactions were carried out in 25 µL using MyTaq™. Cycles were according to Sharma & Giribet (2009) using annealing temperature of 46º Celsius. Unpurified products were sequenced at the Instituto de Biología (LaNaBio), UNAM. Chroma-

tograms and sequences were viewed and edited in Geneious v. 9.1.2 (Kearse et al. 2012). The sequences were examined for stop codons using BLASTX web interface provided by NCBI (Madden 2003) and subsequently uploaded to GenBank for generation of accession number (Electronic Supplement 1). After editing, sequences were attached in a matrix in fasta format through Mesquite v. 3.2 (Maddison & Maddison 2015). COI sequences were aligned using MUSCLE on-line (Edgar 2004). To select the evolutionary model, we compared the results obtained through jModelTest v. 2.1.7 (Darriba et al. 2012) and Partition Finder v. 1.1.1 (Lanfear et al. 2012), the latter considering the gene partitioned by codon position. We selected the model GTR + I + G for Maximum Likelihood analysis, and the models K80 + I, F81 + I and TrN + G for each codon position partition for Bayesian Inference (Electronic Supplements 2 and 3).

2.3. Phylogenetic methods

Outgroup selection for the phylogenetic analysis was based on a previous phylogenetic hypothesis for Stygnopsidae taxa from Cruz-López & Francke (2017). These taxa are the Karosinae *Karos barbarikos* (Genbank accession number KY097819.1) and the two Stygnopsinae *Hoplobunus barretti* (KY097812.1) and *Mexotroglinus* aff. *sbordonii* (KY097821.1). Phylogenetic trees were reconstructed using Maximum Likelihood (ML) and Bayesian Inference (BI). ML analysis was conducted in RaxML-HPC v. 8.0 (Stamatakis 2014) considering 1,000 bootstrap replicates. BI was conducted in Mr. Bayes v. 3.2.6 on XSEDE (Ronquist & Huelsenbeck 2003), consisting of two simultaneous runs each, with four chains default for 30,000,000 generations, sampling every 2,000 trees and the initial 25% of sampled trees were discarded as burn-in. Stationary parameters were viewed in TRACER v. 1.6 (Rambaut et al. 2014). Both analyses were carried out through the on-line portal CIPRES gateway (Miller et al. 2010).

2.4. Molecular dating

Divergence times were estimated using BEAST v2.4.8 (Drummond et al. 2012). Since no stygnopsid or related gonyleptoid fossils are known as well as no timed geological studies on the genesis of the Huautla Cave System (indirect evidence presumes to be very old: Vignoli & Prendini 2009; Steele & Smith 2012; Santibañez-Lopez et al. 2014), BEAST analyses were conducted with COI data partitioned by codon position with a model HKY + I + G for 1st and 2nd positions and GTR + G for 3rd positions. The tree and clock models (but not the site model) were linked across partitions, we used a strict clock with a log normal prior distribution and a Birth Death model process as tree prior. We set the *ucld.mean* of the clock model to a COI rate mutation of 0.0178 substitutions/site/myr (COI clock rate of 3.54% per million years), which

is a well-accepted arthropod clock rate according to Papadopoulou et al. (2010). The analysis ran for 9×10^7 generations, with the initial 20% discarded as burn-in and the effective sample sizes were checked using TRACER. Trees were computed with TREEANNOTATOR v. 1.8.4 (Electronic Supplement 4). Tree annotations, editing and manipulation were done on the R package strap (Bell & Lloyd 2015).

2.5. Molecular species delimitation and haplotypes network

First, we estimated uncorrected genetic distances using MEGA v. 7.0 (Kumar et al. 2016) among the lineages of *Minisge* (Electronic Supplement 5). Also in MEGA we calculated matrix statistics as percentage of variable sites, conserved sites, genetic content and transition/transversion ratios (ti:tv) (Table 1). In addition, we constructed haplotype network using the TCS method (Clement et al. 2000) in PopART v. 1.7 (Leigh & Bryant 2015). For molecular species delimitation, we used three methods: 1) the Automatic Barcode Gap Discovery (ABGD) (Puillandre et al. 2012) using both uncorrected and K2P distance matrices with default options through the on-line version; 2) Generalized Mixed Yule Coalescent (GMYC) (Pons et al. 2006) with a single threshold through on-line portal using the ultrametric tree obtained from the BEAST dating analysis; and 3) Bayesian Poisson Tree Process (bPTP) (Zhang et al. 2013) using the same tree from the BEAST analysis, thinning every 1,000 and removing outgroup taxa, discarding the first 25% of generations as burn-in (Electronic Supplements 6–9).

3.   Results

3.1.   Taxonomy

Order Opiliones Sundevall, 1833
Suborder Laniatores Thorell, 1876
Superfamily Gonyleptoidea Sundevall, 1833
Family Stygnopsidae Sørensen, 1932
Subfamily Stygnopsinae Sørensen, 1932

3.1.1. *Minisge* gen.n.
Figs. 2–7

Type species. *Minisge sagai* sp.n.

Composition. *Minisge kanoni* sp.n. and *Minisge sagai* sp.n.

Considerations on nomenclature of macrosetae of penis. According to Cruz-López & Francke (2017), stygnopsine harvestman usually do not have macrosetae E, only the genera *Paramitraceras* Pickard-Cambridge, 1905, *Philora* Goodnight & Goodnight, 1954, *Sbordonia* Šilhavý, 1977 and *Troglostygnopsis* Šilhavý, 1974

exhibit two pairs of macrosetae E on ventral side of pars distalis, and the macrosetae E1 pair is always small. *Hoplobunus* Banks, 1900 is another genus that exhibits a small pair of E1 setae. Based on the similarity criterion (small E1), we assume that the macrosetae E are absent in the remaining stygnopsine genera; for that reason, we hypothesise herein that *Minisge* only has large macrosetae C along the lateral margins towards the ventral side.

Description. Troglomorphic stygnopsine, femur IV straight and longer than scutum. Ocularium at the frontal margin of scutum, narrow and conical, armed with long apical spine. Scutum type zeta (ζ), mid-bulge slightly convex. Mesotergal area V with median acute spine, almost as high as ocularium. Trochanter III sub-cylindrical. Chelicera sexually dimorphic, larger in males. Cheliceral dentition heterogeneous, movable finger with basal tooth blunt. Posterior legs with two ventral rows of spiniform tubercles, increasing in size distally. Pars distalis of penis spoon-shaped, follis on meso-apical depression. Penial macrosetae *Stygnopsis*-pattern, with the following arrangement: 4–5 pair of macrosetae C forming a longitudinal row, from ventral side to near the base of follis; 2 pairs of both macrosetae A and B on lateral sides of pars distalis, basal to meso-apical depression; 1 pair of small macrosetae D at base of follis. Females are similar to males, but with the chelicera smaller and armature on legs less developed.

Differential diagnosis. *Minisge* can be differentiated easily from other troglomorphic stygnopsine by the presence of an acute long spine on mesotergal area V. General aspect of this new genus is similar to that of *Iztlina* Cruz-López & Francke, 2017, *Serrobunus* Goodnight & Goodnight, 1942, and *Tonalteca* Cruz-López & Francke, 2017, but differs from these by the dorsal armature on scutum, the macrosetal arrangement on penis, and the absence of mono- or bilobular dorsal projection on follis.

Variation. Within each species, there is little morphological variation. *M. kanoni* exhibits a minor variation on cuticular coloration, specimens from Linita, La Grieta and Skull cave are lighter than remaining specimens. Among *M. sagai* specimens, only a few males exhibit a minor variation in cheliceral size.

Distribution. This genus is endemic to the Huautla Cave System, Oaxaca, Mexico.

Natural history. All specimens of *Minisge* were collected walking along walls of the caves, and were also found under rocks inside the caves. Sometimes small aggregations were present, formed by 4 or 5 specimens. *M. sagai* was found from few meters from the entrance of each cave to at most 200 m deep; whereas *M. kanoni* was found in the deeper areas of the caves, from about 400 m to 600 m.

Derivatio nominis. An anagram referring to the fictitious Gold Saint of the constellation Gemini (Geminis in Spanish) in the Japanese anime of Saint Seiya. It is used as a noun in apposition; gender masculine.
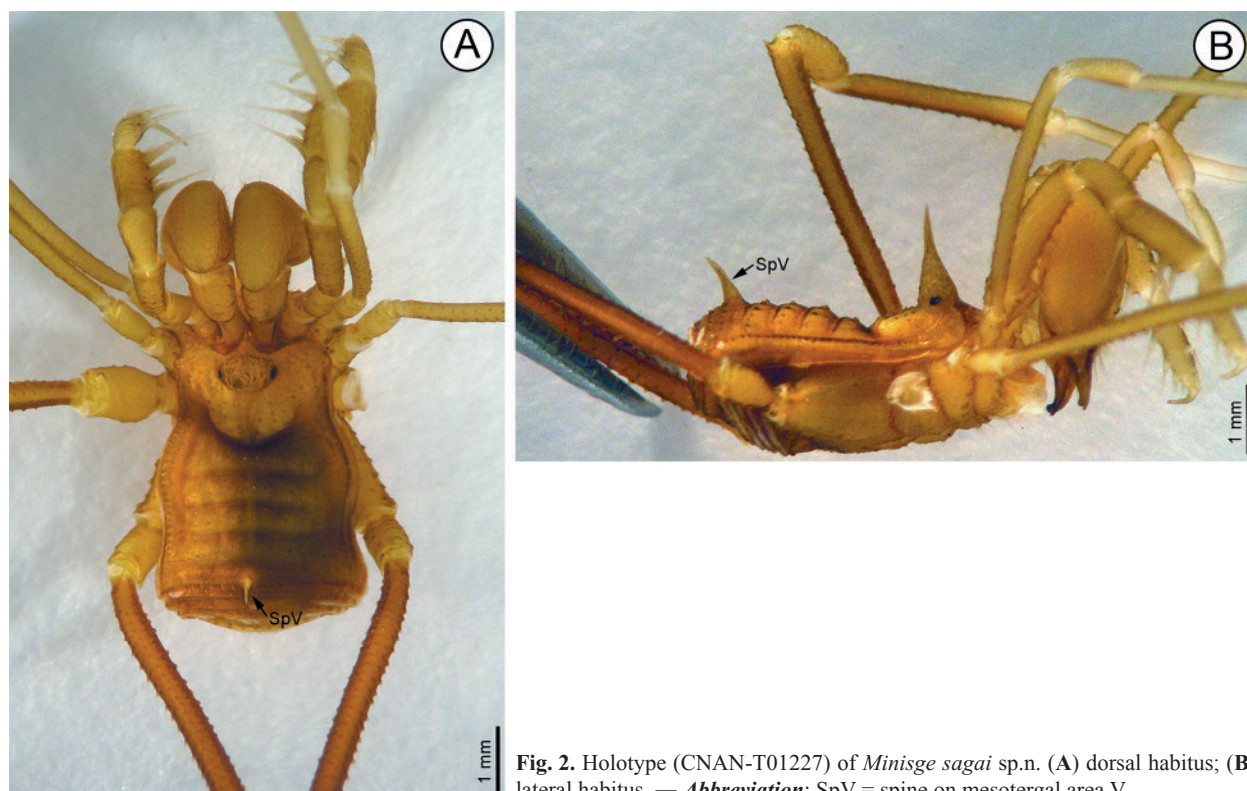
Fig. 2. Holotype (CNAN-T01227) of *Minisge sagai* sp.n. (**A**) dorsal habitus; (**B**) lateral habitus. — *Abbreviation*: SpV = spine on mesotergal area V.

3.1.2. *Minisge* sagai sp.n.
Figs. 2–4

Type material. Holotype ♂CNAN-T01227 (DNA-Op0096) from Mexico, Oaxaca, Huautla de Jiménez, Millipede cave, 18°07′03.10″N 96°47′59.38″W, 14 April 2015, Colls. O. Francke et al. 1♂ 1♀ **paratypes** CNAN-T01228 (DNA-Op0097, SEM-Op228) from Mexico, Oaxaca, Huautla de Jiménez, Millipede cave, 18°07′03.10″N 96°47′59.38″W, 09 April 2015, Colls. O. Francke et al. 2♂ 1♀ **paratypes** CNAN-T01229 (DNA-Op166, 167, 168) from Mexico, Oaxaca, Huautla de Jiménez, La Grieta cave, 18°08′17.34″N 96°47′23.85″W, 09 April 2015, Colls. O. Francke et al. 1♂ **paratype** CNAN-T01230 (DNA-Op144) from Mexico, Oaxaca, Huautla de Jiménez, Skull cave, 18°06′38.88″N 96°47′53.23″W, 11 April 2015, Colls. O. Francke et al. 6♂ 5♀**paratypes** CNAN-T01231 (DNA-Op108, 113, 115, 117, 120) from Mexico, Oaxaca, Huautla de Jiménez, Río Iglesia cave, 18°07′03.10″N 96°47′59.38″W, 13 April 2014, Colls. O. Francke et al. 3♂ **paratypes** CNAN-T01232 (DNA-Op127, 128, 129) from Mexico, Oaxaca, Huautla de Jiménez, Inclined cave, 18°06′24.48″N 96°47′58.52″W, 14 April 2015, Colls. O. Francke et al. 1♂ 1♀ **paratypes** CNAN-T01233 (DNA-Op146, 147) from Mexico, Oaxaca, Huautla de Jiménez, Sump cave, 18°06′26.00″N 96°47′54.49″W, 11 April 2015, Colls. O. Francke et al. 2♂ 2♀ **paratypes** CNAN-T01234 (DNA-Op102, 103, 104, 105) from Mexico, Oaxaca, Huautla de Jiménez, Small Pit cave, 18°08′15.86″N 96°46′59.01″W, Colls. O. Francke et al.

Differential diagnosis. Reddish color, eyes present and well-marked, pigmented. Ratio of femur IV length / scutum length < 2.0. Apical portion of pars distalis not swollen, similar in width along the pars distalis, basal constriction faint. 5 pairs of macrosetae C (setae C1 – C5) forming a continuous, evenly spaced row; all macrosetae C separated from each other by the same distance.

Derivatio nominis. Patronymic dedicated to Saga, the older twin who wears the golden cloth of Gemini, in the Japanese anime of Saint Seiya.

Description. *Dorsum* (Figs. 2, 3E): scutum length: 4.4 mm. Scutum type ζ, constrictions I and II shallow, coda slightly rounded. Ocularium at the frontal margin of prosoma, with base elliptical and very high, apically with a long acute spine, with many posterior rows of small tubercles forming a "V". Eyes at base of ocularium, dark and well defined. Dorsum smooth, each mesotergal area with a transversal row of 8–10 pairs of small tubercles, mesotergal sulci pronounced. Posterior margin of mesotergal area V with a median, long and acute spine, slightly lower than the ocularium. *Venter* (Fig. 3A): coxae I–III with spiniform setiferous tubercles, longer on coxae I, decreasing in size to coxae III. Coxae IV slightly larger than coxae III, ornate with few small setiferous tubercles. Lateral margins posterior to genital operculum constrained at the base. *Chelicera* (Fig. 3B,C): basichelicerite elongated, with the bulla swollen dorsally. Cheliceral hand very swollen, dorsal portion elevated over junction with the basichelicerite. Frontal face of cheliceral hand with small spiniform tubercles and spiniform setae. Fixed finger with 8 teeth, the median and apical ones bigger than the basal. Movable finger with a large basal blunt tooth and a row of four flat teeth. *Pedipalp* (Fig. 3D): trochanter globular, basally with a long spiniform tubercle. Femur slightly compressed laterally, dorsally ornate with few small tubercles, ventrally with a row of 10 spiniform tubercles throughout length of segment, the apical 7 tubercles close to each other, basal-most largest. Patella sub-cylindrical, ornate with few spiniform tubercles. Tibia and tarsus armed with long spiniform setiferous tubercles as follows: mesal tibia IiII (4 > 3 >1 > 2), ectal tibia IiiII (4 > 1 > 5 > 3 > 2); both margins of tarsus: III (1 > 2 > 3). Tarsal claw as long as tarsus.
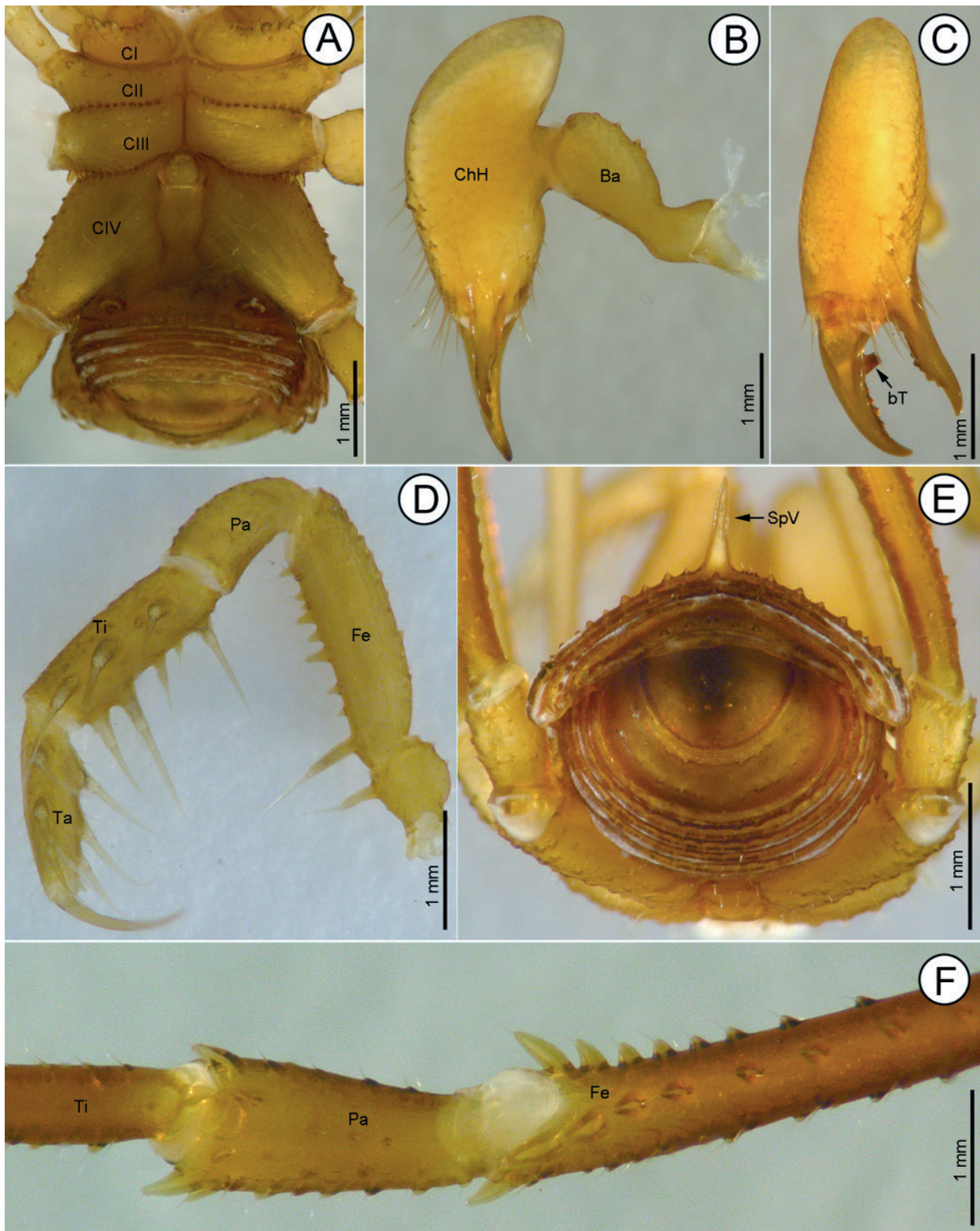
Fig. 3. Paratype male (CNAN-T01231) of *Minisge sagai* sp.n. (**A**) ventral view of body; (**B**) mesal view of right chelicera; (**C**) frontal view of right chelicera; (**D**) mesal view of right pedipalp; (**E**) posterior view body; (**F**) ventro-lateral view of right patella IV. — ***Abbreviations***: Ba = basichelicerite, bT = basal tooth of movable finger, CI–CIV = coxae I–IV respectively, ChH = cheliceral hand, Fe = femur, Pa = patella, SpV = spine on mesotergal area V, Ta = tarsus, Ti = tibia.

Legs: Length femur IV 8.0 mm, ratio femur IV length / scutum length 1.8. All segments long and slender. Femora to tibia covered by spiniform tubercles, metatarsi and tarsi covered by spiniform setae. Femora to tibia III and IV with 2 ventral rows of spiniform tubercles, increasing in size distally and more prominent at the end of these segments (Fig. 3F). Tarsal count: 9(3):27(4):7:8, first basitarsomeres of legs III and IV very long, > 3 × length of second basitar-
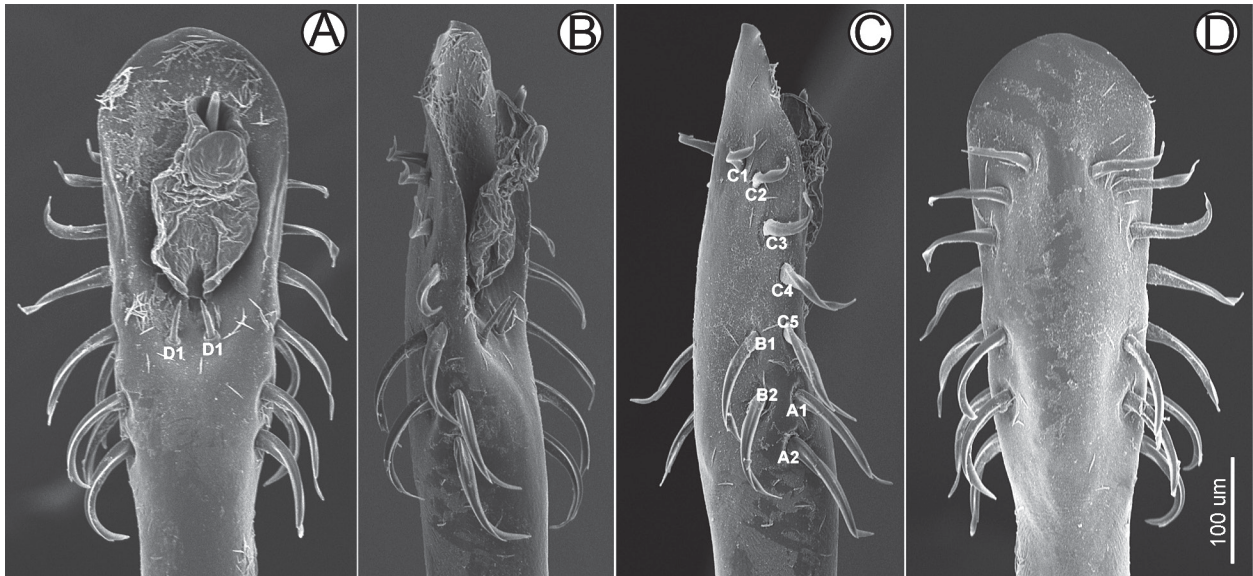
Fig. 4. Male genitalia of paratype male (CNAN-T01228) of *Minisge sagai* sp.n. (**A**) dorsal view; (**B**) laterodorsal view; (**C**) lateral view; (**D**) ventral view. — **Abbreviations**: A1, A2, B1, B2, C1, C2, C4, C5, D1 = respective macrosetal groups on penis. — Scale bar on (D) valid for all figures.
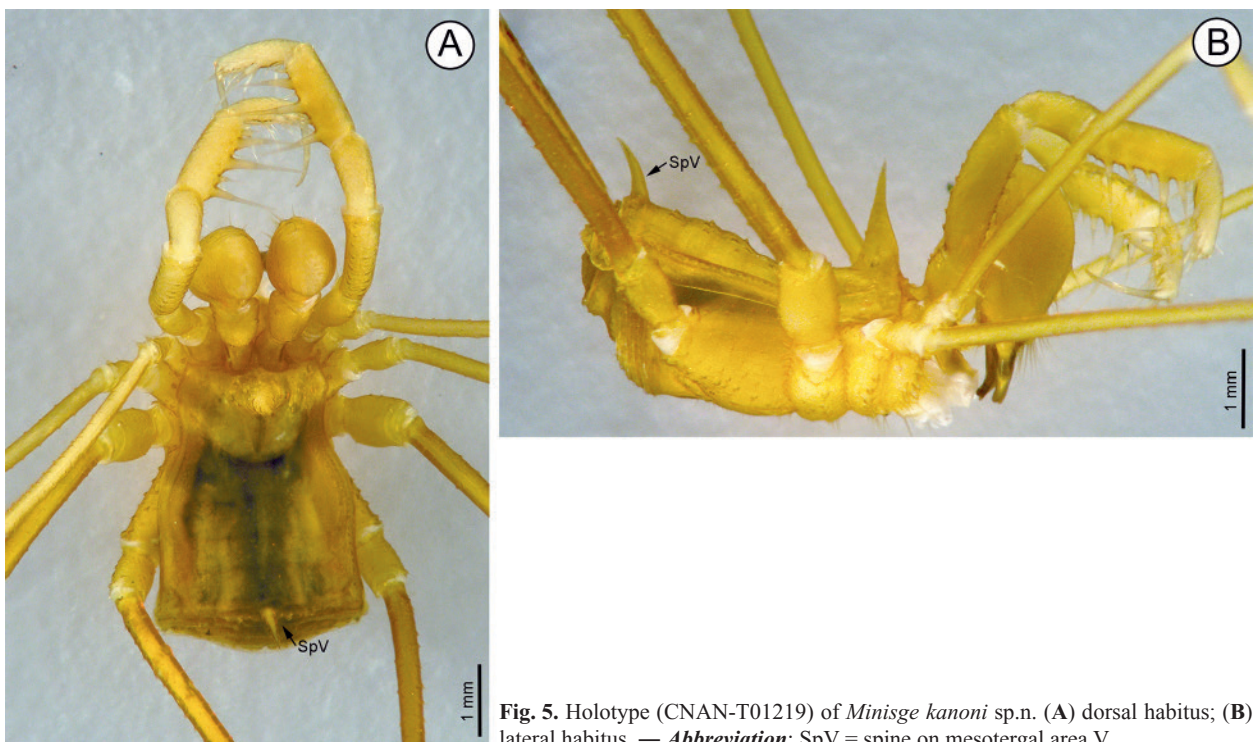

Fig. 5. Holotype (CNAN-T01219) of *Minisge kanoni* sp.n. (**A**) dorsal habitus; (**B**) lateral habitus. — **Abbreviation**: SpV = spine on mesotergal area V.

someres. **Penis** (Fig. 4): pars distalis with subtle basal constriction and with mesoapical depression, flimsy lamina not swollen and apically rounded. All macrosetae of penis very large and with a longitudinal furrow, except macrosetae D1 being shorter than remaining setae and without furrow. 5 pairs of macrosetae C, contiguous and separated from each other by the same distance; C1 and C2 slightly displaced to the ventral side. 2 pairs of macrosetae A and B, macrosetae B slightly displaced to the ventral side. 1 pair of macrosetae D1 dorsally at the base of follis. Follis multifolded, with the stylus inserted in it.

3.1.3. *Minisge kanoni* sp.n.
Figs. 5 – 7

Type material. ♂ **holotype** CNAN-01219 (DNA-Op0095) from Mexico, Oaxaca, Huautla de Jiménez, Li Nita cave, 18º08′17.34″N 96º47′23.85″W, 12 April 2012, Colls. O. Francke et al. 1♀ **para-type** CNAN-T01220, same data as the holotype, but 10 April 2012. 2♂ **paratypes** CNAN-T01221 (SEM-Op229), same data as the holotype, but 11 April 2016. 1♂ 1♀ **paratypes** CNAN-T001222 (DNA-Op0100, Op0101) from Mexico, Oaxaca, Huautla de Jiménez, Basketball cave, 18º08′17.44″N 96º46′01.81″W, 14 April 2014, Colls. O. Francke et al. 1♀ **paratype** CNAN-T01223 (DNA-Op0145) from Mexico, Oaxaca, Huautla de Jiménez, Skull
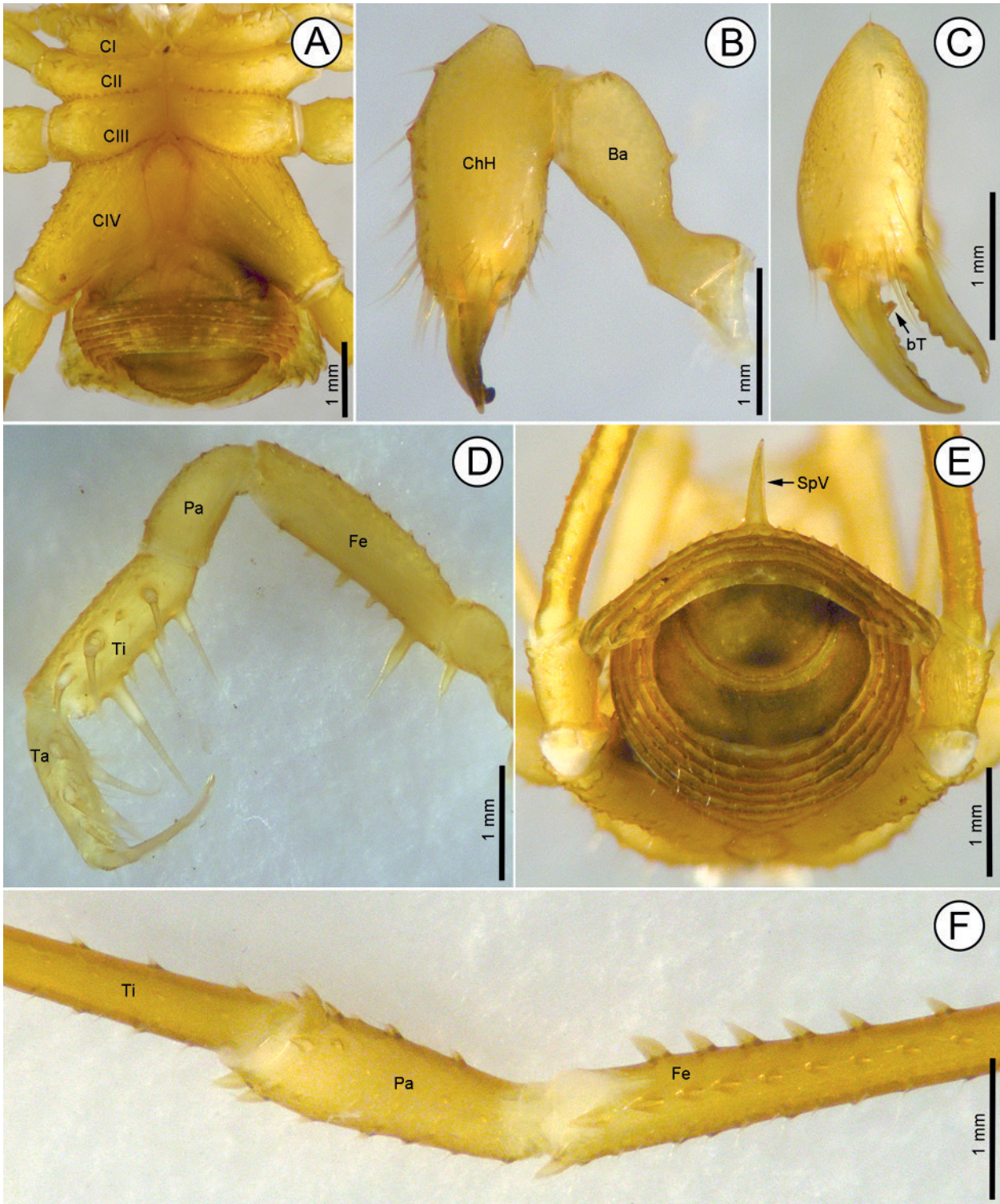
Fig. 6. Paratype male (CNAN-T01221) of *Minisge kanoni* sp.n. (**A**) ventral view of body; (**B**) mesal view of right chelicera; (**C**) frontal view of right chelicera; (**D**) mesal view of right edipalp; (**E**) posterior view body; (**F**) ventro-lateral view of right patella IV. — ***Abbreviations***: Ba = basichelicerite, bT = basal tooth of movable finger, CI–CIV = coxae I–IV respectively, ChH = cheliceral hand, Fe = femur, Pa = patella, SpV = spine on mesotergal area V, Ta = tarsus, Ti = tibia.

cave, 18º06′38.88″N 96º47′53.23″W, 11 April 2015, Colls. O. Francke et al. One male, 1♀ 1 juvenile **paratypes** CNAN-T01224 (DNA-Op0165) from Mexico, Oaxaca, Huautla de Jiménez, La Grieta cave, 18º08′17.34″N 96º47′23.85″W, 9 April 2015, Colls. O. Francke et al. 1♂ 7♀ 1 juvenile **paratypes** CNAN-T01225 (DNA-Op107, Op110, Op114, Op121, Op122, Op125) from Mexico, Oaxaca, Huautla de Jiménez, Río Iglesia cave, 18º07′03.10″N

96º47′59.38″W, 13 April 2014, Colls. O. Francke et al. 1♂ **paratype** CNAN-T01226 (DNA-Op126) from Mexico, Oaxaca, Huautla de Jiménez, Inclined cave, 18º06′24.48″N 96º47′58.52″W, 14 April 2015, Colls. O. Francke et al.

Differential diagnosis. Pale yellow color, eyes reduced and almost absent, unpigmented. Ratio of femur IV
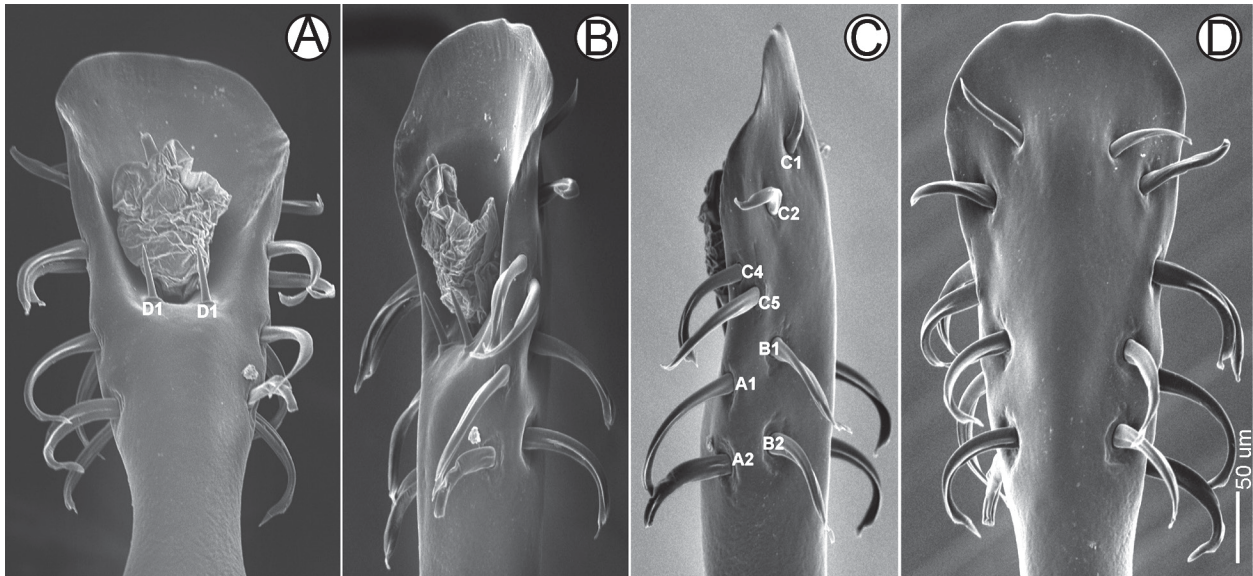
Fig. 7. Male genitalia of paratype male (CNAN-T01221) of *Minisge kanoni* sp.n. (**A**) dorsal view; (**B**) laterodorsal view; (**C**) lateral view; (**D**) ventral view. — *Abbreviations*: A1, A2, B1, B2, C1, C2, C4, C5, D1 = respective macrosetal groups on penis. — Scale bar on (D) valid for all figures.

length / scutum length > 2.5. Apical portion of pars distalis swollen and with a noticeable basal constriction. 4 pairs of macrosetae C (setae C3 absent), a distinct gap between the 2 basal-most (C4, C5) and the 2 distal-most pairs (C1, C2); C4 and C5 very near to each other.

Derivatio nominis. Patronymic dedicated to Kanon, the younger twin who wears the Golden cloth of Gemini in the Japanese anime of Saint Seiya.

Description. *Dorsum* (Figs. 5, 6E): scutum length 4 mm. Scutum type ζ, constrictions I and II shallow, coda slightly pronounced. Ocularium at the frontal margin of prosoma, with base elliptical and very high, apically with long acute spine. Eyes at base of ocularium, poorly marked and small. Dorsum smooth, each mesotergal area with a transversal row of 5–6 small tubercles, mesotergal sulci shallow. Posterior margin of mesotergal area V with a median, long and acute spine of the same height as the ocularium. *Venter* (Fig. 6A): coxae I–III similar in size, ornate with spiniform setiferous tubercles, longer on coxae I. Coxae IV slightly larger than coxae III, ornate with small setiferous tubercles. Lateral margins posterior to genital operculum constrained at the base. *Chelicera* (Fig. 6B,C): basichelicerite elongated, with the bulla swollen dorsally. Cheliceral hand slightly swollen, dorsal portion slightly elevated over junction with the basichelicerite. Frontal face of cheliceral hand with small spiniform tubercles and spiniform setae. Fixed finger with 7 teeth, increasing in size apically. Movable finger with basal tooth blunt and a row of 5 flat, contiguous teeth. *Pedipalp* (Fig. 6D): trochanter globular, basally with a long spiniform tubercle. Femur slightly compressed laterally, dorsally ornate with few small tubercles, ventrally with a row of 6 spiniform tubercles extending throughout the length, the basal-most largest. Patella sub-cylindrical, ornate with few spiniform

tubercles. Tibia and tarsus armed with long spiniform setiferous tubercles as follows: mesal tibia IiII (3 > 1 = 4 > 2), ectal tibia IIiI (4 > 1 = 2 > 3); both margins of tarsus: III (1 > 2 > 3). Tarsal claw as long as tarsus. *Legs*: Length femur IV 10.8 mm, ratio femur IV length / scutum length 2.7. All segments long and slender. Femora to tibia covered by spiniform tubercles, metatarsi and tarsi covered by spiniform setae. Femora to tibia IV with 2 ventral rows of spiniform tubercles, increasing in size distally and more prominent at the end of these segments (Fig. 6F). Tarsal count: 12(4):33(5):7:8, first basitarsomeres of legs III and IV very long, > 3 × length of second basitarsomeres. *Penis* (Fig. 7): pars distalis with a basal constriction and with mesoapical depression, flimsy lamina slightly swollen and apically rounded. All macrosetae of penis very large and with a longitudinal furrow, except macrosetae D1 being shorter than remaining setae and without furrow. 4 pairs of macrosetae C, C3 absent, so there is a gap between C2 and C4; C1 and C2 slightly displaced to the ventral side; C4 and C5 very close to each other. 2 pairs of macrosetae A and B, macrosetae B slightly displaced to the ventral side. 1 pair of macrosetae D1 dorsally on the base of follis. Follis multifolded, with the stylus inserted in it.

3.2. Systematics, molecular species delimitation and divergence

Phylogenetic analyses with ML and BI show similar results with a few differences in nodal support, recovering *Minisge* as a monophyletic group (Figs. 8, 12). In addition, both analyses show minimal diversification within the *M. sagai* lineage, contrasting with the *M. kanoni* lineage, which is conformed by four clades from specimens of different areas of the cave system (Figs. 8, 9).
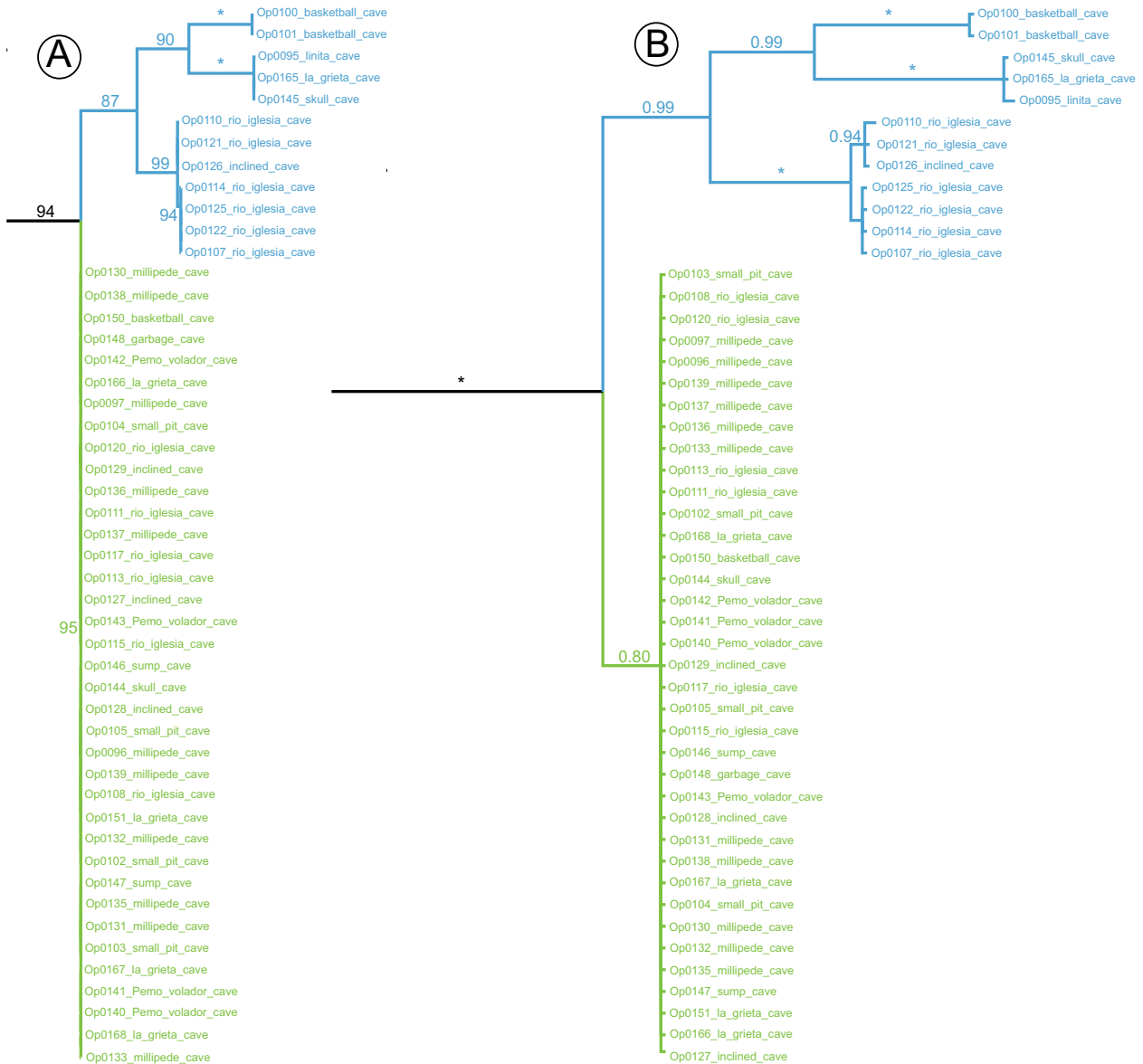
Fig. 8. Phylogenetic relationships among species of *Minisge* gen.n. (**A**) Maximum Likelihood topology; (**B**) Bayesian topology. Lineages of *Minisge kanoni* sp.n. in blue, of *Minisge sagai* sp.n. in green. * = Bootstrap values of 100 (A) and posterior probability values of 1.0 (B).

Species delimitation methods for the COI data used here recognize four (ABGD and GMYC) or six (bPTP) species (Fig. 9), with *M. kanoni* lineage as the most divergent group, divided in three or four different species, corresponding to the major clades in the topology (ABGD and GMYC considering Río Iglesia + Inclined caves as one clade/species).

Additionally, uncorrected genetic distances reveal a divergence of 0% among populations of shallow-inhabiting *M. sagai* (Electronic Supplement 5), which at the same time exhibits a continuous genetic flow across populations from throughout the Huautla Cave System, which is concordant with our phylogenetic hypothesis. On the other hand, populations of deeper-inhabiting *M. kanoni* linage, present variable genetic distances, which range from 0 to 0.2% within each of the four clades (among the different putative species of each clade recovered in the species delimitation analyses). However,

the distances among populations of *M. kanoni* from the Cueva del Rio Iglesia and the other three clades range from 0.6% with Inclined cave, to 10% with Basketball cave and 13% with Li Nita cave. The clades from Li Nita and Basketball caves are considerably different genetically from the clades of Rio Iglesia and Inclined cave, which is concordant with our phylogenetic analysis and the species delimitation methods used.

Furthermore, the genetic distances between the two species of *Minisge* recognized here based on morphology, go from 9.3% in the two populations within Rio Iglesia cave to 13.1% in the two populations within Li Nita cave, which are the populations with more mutations in their haplotypes (Electronic Supplement 5).

Simultaneously, the results obtained with the species delimitation methods and the genetic distances are concordant with the haplotype network analyses, which recover one network with six different haplotypes for
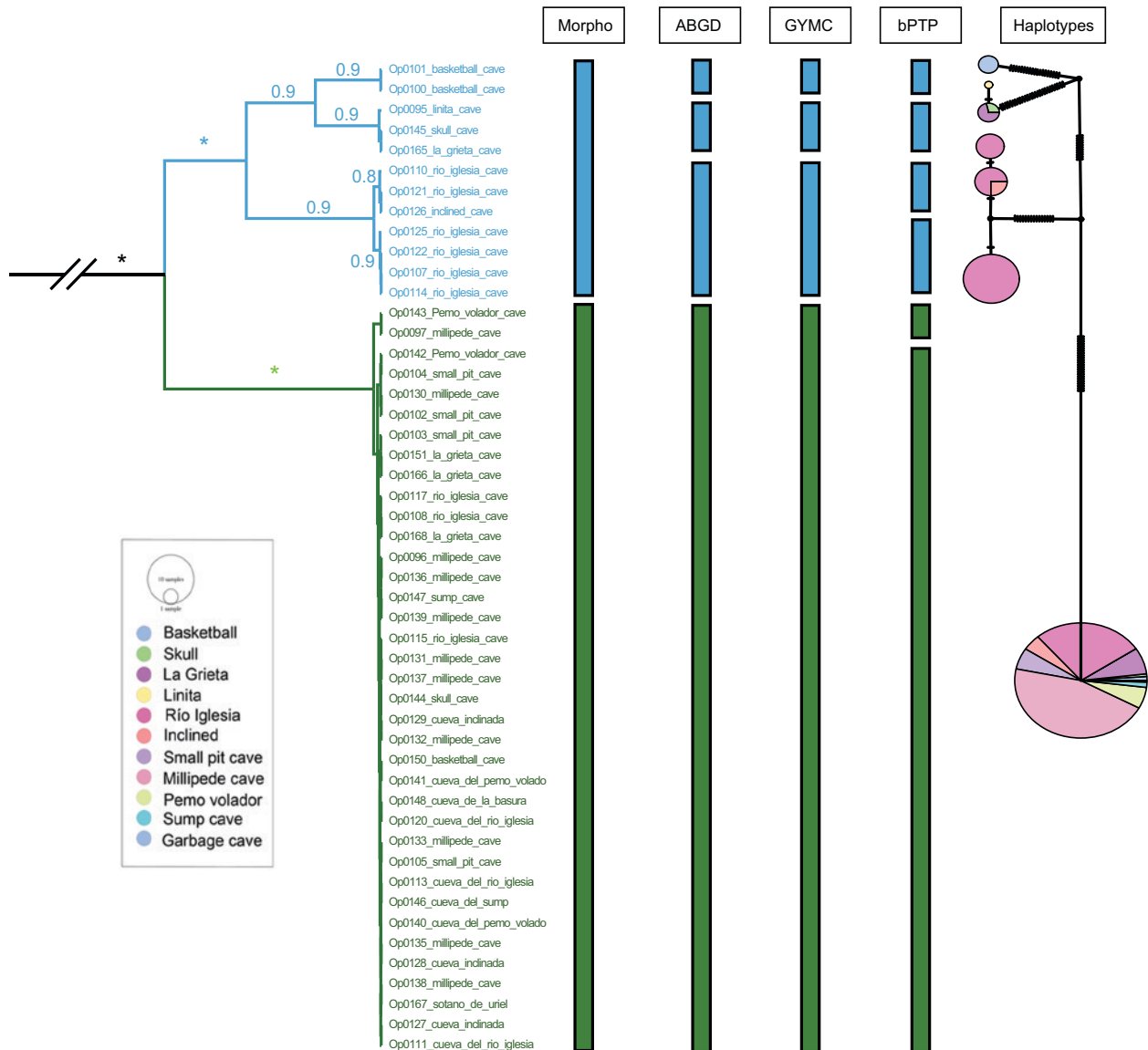
Fig. 9. Delimitation of species of the lineages of *Minisge* gen.n. obtained under different methods: Morphology, ABGD, GMYC and bPTP. Lineages of *Minisge kanoni* sp.n. in blue, of *Minisge sagai* sp.n. in green. * = posterior probability values of 1.0. Haplotype network obtained using PopArt.

M. kanoni and only one haplotype for *M. sagai* (Fig. 10). Thus, networks suggest that *M. sagai,* the shallow inhabiting species, moves freely among the cave entrances in the Huautla System, probably over the surface, although we have never collected it outside the caves. Haplotypes of *M. sagai* and *M. kanoni* are differentiated by 21 mutations, which is also concordant with our morphological species results. *M. kanoni* lineage is conformed by three different haplotypes for Rio Iglesia + Inclined caves (upper left in Fig. 10), separated from each other by a single mutation; the former differing by 15 mutations from the rest of the haplotypes; this lower branch splits in two: Basketball cave, which differs by 19 mutations from its nearest relatives, and La Grieta + Skull + Li Nita caves sharing 26 unique mutations among them, with Li Nita population differing from La Grieta + Skull caves by one mutation. The haplotype network analysis supports the structure recovered with ABGD and GMYC species de-

limitation analyses; however, because we are unable to morphologically distinguish among the various deep-inhabiting populations we prefer to retain them as a single species. In concordance, the COI analysis of variable and conserved sites shows that populations of *M. sagai* are conserved, without variation, whereas, the major variation observed in *M. kanoni* (40%) is located on the third codon position, which is related at the same time with the values of ti:tv ratio for COI = 5.8 (Table 1), suggesting that the data is not under considerable saturation; therefore, the genetic differences are mostly due to silent mutations, and this re-enforces our decision to recognize all populations of *M. kanoni* as belonging to the same species.

Finally, molecular dating of *Minisge* indicated that the two species of the genus diverged approximately 3.9 Mya (95% HPD: 3.1–4.9), with the intraspecific radiation of deep-inhabiting *M. kanoni* occurring about
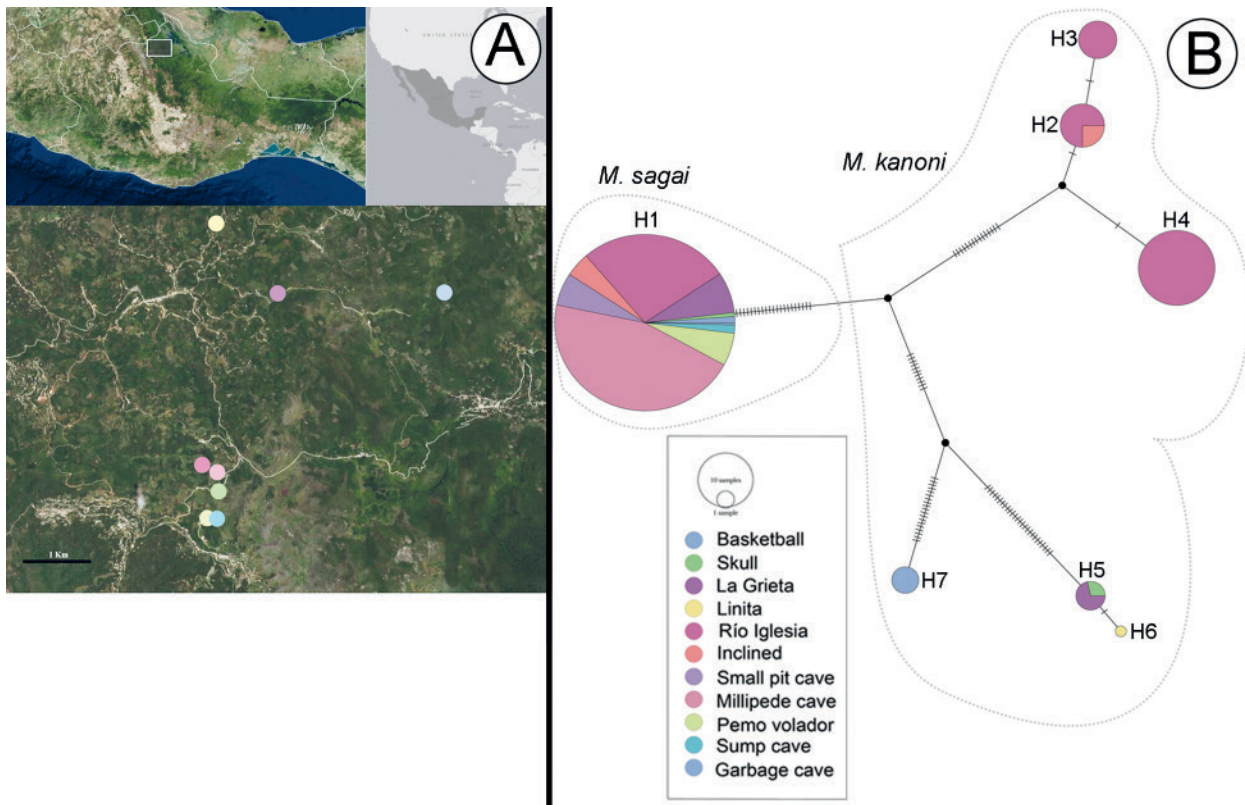
Fig. 10. Huautla Cave System maps and haplotype network: (**A**) map of Huautla Cave System region, showing the sampled caves. (**B**) Haplotype network obtained using PopArt. Color legends of the sampled caves in the inset on haplotype network, the haplotypes are indicated with H1–7 respectively, dotted grey lines indicate both species of *Minisge*. Some caves in (A) are not shown because many caves share the same geographical coordinates.

3.3 Mya (95% HPD: 2.6–4.2), and the intraspecific radiation of shallow-inhabiting *M. sagai* occurring very recently, as most branches shown in the dated chronogram are unsupported (Fig. 12A).

4. Discussion

4.1. Speciation within caves

Caves are complex environments where the conditions that allow the colonization and establishment of the species depend on multiple variables including humidity, temperature, airflow, and the amount of organic matter that goes into the cave (SIMON 2012). Many of those conditions are associated with the genesis, shape and depth of the caves. Thus, the conditions at the entrance, compared with the conditions in very deep areas of the cave will differ significantly, as well as with those caves with high intakes of water or organic matter (GALAN & HERRERA 1998). These conditions may or may not affect the distribution of the individuals within the cave, but we would expect that in a cave system without apparent physical barriers between the cave branches, a population with many individuals would be able to move throughout and colonize the entire system. However, and as is shown in

Table 1. Length of COI marker for the alignment of *Minisge* species, indicating number and percentage of variable and conserved sites among the gene fragment sequenced, and partitioned by codon positions. — ***Abbreviations***: ti = transitions, tv = transversions.

	COI	%	1st	%	2nd	%	3rd	%
Minisge								
Length	507		169		169		169	
Variable	88	17	7	4	1	1	80	47
Conserved	419	83	162	96	168	99	89	53
ti : tv	5.8		2.5		0		6.6	
M. sagai								
Length	507		169		169		169	
Variable	0	0	0	0	0	0	0	0
Conserved	507	100	169	100	169	100	169	100
ti : tv	0.53		0.4		0.7		0.5	
M. kanoni								
Length	507		169		169		169	
Variable	72	14	5	3	0	0	67	40
Conserved	435	86	164	97	169	100	102	60
ti : tv	48.1		474.9		0.7		80.3	

our results, the particular case of *Minisge* is apparently an exception, a situation where the cave conditions are shaping and moulding a complex population structure. *Minisge sagai* is restricted to the upper area of the Huautla Cave System, inhabiting all cave entrances explored,
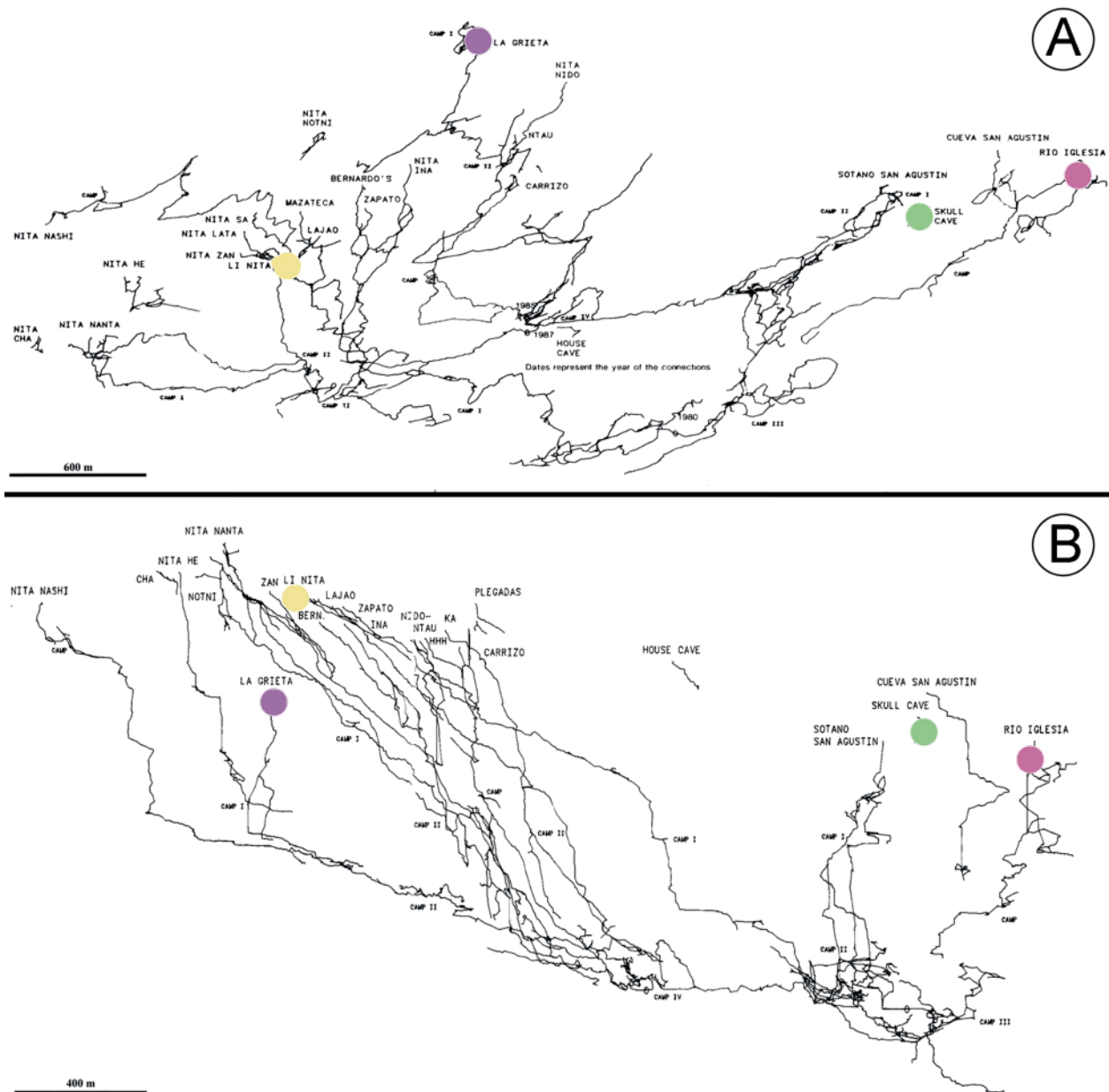
Fig. 11. Topographic (**A**) and profile map (**B**) of the main caves of the Huautla System. Color legends of the sampled caves are the same of the haplotype network of Fig. 10. Note: not all caves are indicated in the figures because they shared the same geographical coordinates. Topographic and profile maps modified from PESH web page (www.peshcaving.org).

despite the uneven landscape of the Sierra Mazateca, which suggests that individuals of *M. sagai* are moving between the caves, although the species has not been collected in epigean habitats. However, we must point out that the sampling effort was restricted to three consecutive Aprils (the dry season), since it is the best time of the year for cave exploration, and the dry season might not be the most suitable time for these tiny harvestmen to move on the surface. In addition, the near absence of juveniles in our samples suggests that the breeding season might be associated with the wet season, and for those reasons, we have not collected *M. sagai* outside the caves.

In contrast, specimens of *M. kanoni* where collected in almost all caves explored by us, at an intermediate depth, about ~ 100 m from the surface in La Grieta and Li Nita to about ~ 500 m in Río Iglesia cave, even though the difference in elevation between their entrances is over 300 m (Fig. 10D). Surprisingly, one of the four clades of *M. kanoni* shows specimens of Skull cave as sister to one from La Grieta cave, even though these caves are 3.1 km apart in a straight line and are separated by the Iglesia River. Also, in the lineages of *M. kanoni*, the clade of Río Iglesia + Inclined caves are sister to La Grieta + Li Nita + Basketball caves (excluding Skull cave), these two clades are in the southern and the northern part of the mountain range, respectively, divided by the Iglesia River.

The morphology of *M. kanoni* suggests a more accentuated adaptation to the caves (lack of pigmentation, eyes reduced or absent, elongation of appendages), perhaps

because it is confined to deeper parts of the cave system since diverging from its sister species. However, genetic distances and haplotypes of *M. kanoni* show a more complex population structure, reflected in our haplotype network and the number of mutations among different haplotypes, which suggests that populations of *M. kanoni* are in constant genetic diversification. Our inability to recognize and distinguish morphologically the genetic species within *M. kanoni* could be due to the similaritys in the deeper cave environment mentioned previously.

The deepest areas of the system converge at a depth of about ~ 800 m, which is the part of the system that becomes horizontal, with deep water pools and sumps, and where the blind scorpion *Alacran tartarus* Francke, 1982 inhabits and can move up and down throughout the system. Conversely, the middle areas of the system appear to be more isolated from each other (Fig. 10D, 11). Specimens of *M. kanoni* have been seldom collected in the deepest portions of the system, they remain in the middle portions of the caves, suggesting that they do not disperse through the deep tunnels in the connected deeper area of the system, which suggest that populations are currently isolated, and thus more genetic mutations can be seen in the different populations of *M. kanoni* as shown in the haplotype networks.

4.2. Species delimitation

Molecular species delimitation based on COI has been used in several groups of arthropods (HEBERT et al. 2003, 2004), even in some groups of armoured harvestmen (THOMAS & HEDIN 2008; DERKARABETIAN et al. 2010, 2011; FERNÁNDEZ & GIRIBET 2014). In those works, the North American species *Fumontana deprehendor* Shear, 1977 and *Sclerobunus robustus* (Packard, 1877), and the New Zealand *Aoraki denticulata* (Forster, 1948), show little morphological differentiation and high genetic diversification, yielding 5, 6 or even 28 putative species, respectively. The genetic *p*-distance between COI haplotypes of up to 21.98% in *A. denticulata* is remarkable (THOMAS & HEDIN 2008; DERKARABETIAN et al. 2010, 2011; FERNÁNDEZ & GIRIBET 2014). These examples of incongruence between morphological and genetic diversification has been interpreted as a highly conserved morphology associated with conserved microhabitat preference, process known as niche conservatism (WIENS & GRAHAM 2005; DERKARABETIAN et al. 2011). Based on this, we could speculate that the lack of morphological differentiation of the genetic lineages in *M. kanoni*, could be associated with the similarity in environmental conditions in the deeper areas in the caves, as mentioned before. Therefore, we prefer to recognise only two species within the Huautla Cave System, but to highlight the evidence of diversification and the amount of mutations observed in *M. kanoni* by the delimitation and haplotype networks analyses. Additionally, the analysis of the percentage of variable and conserved sites, among *M. sagai* exhibit no variation between all codon positions, however, the

third positions in *M. kanoni* shows 40% of variation, this value plus the high value for the ti:tv ratio = 48.1 indicates that the largest majority differentiation among the four clades of *M. kanoni* are due to changes on the third codon position, the data is not suffering of saturation and thus, these genetic changes are dominated by transitions instead of transversions. These genetic changes are possibly by synonymous mutations on COI, so our molecular results are different from the morphological species delimitation in this study (Table 1). The morphology of *M. kanoni* is very conserved and it has proven impossible to differentiate among populations, and since we are here describing the species based on morphology, we prefer to recognize one species for the shallower portions of the system (*M. sagai*) and one species for the deeper portions of the system (*M. kanoni*).

4.3. Colonization and diversification

Molecular dating shows the diversification of *Minisge* occurred in the Middle Pliocene approximately 3.9 Mya, which is characterized by the drastic climatic changes which impacted the distribution and genetic structure of North America fauna (Fig. 12B), wherein some invertebrates sought hypogean habitats as microrefugia (BARR & HOLSINGER 1985; HEWITT 1996; ZACHOS et al. 2008; JUAN et al. 2010; HANSEN et al. 2013; BRYSON et al. 2014). Some of these microrefugia like caves are a way to find shelter from adverse conditions and has been reported in other arachnid groups like harvestmen and scorpions (GALAN & HERRERA 1998; DERKARABETIAN et al. 2010; BRYSON et al. 2014).

It is remarkable that the intraspecific diversification of deep-inhabiting *M. kanoni* occurred approximately 3.3 Mya, being older than *M. sagai*, demonstrating that *M. kanoni* may have invaded the cave first, having enough time to develop more accentuated troglomorphisms and genetic structure as we discussed above. On the other hand, the lineage of *M. sagai* has not diversified yet, showing only one haplotype, no genetic variation (shown in the genetic distances) and no diversification, suggesting that this species invaded the cave system later (in a second colonization event) occupying areas near to the surface and showing less accentuated troglomorphisms.

The evolutionary history and mechanisms that led *Minisge* to adapt and evolve inside the caves are complex and difficult to explain based on the collection data used in this work. There are several possible scenarios of the evolution of *Minisge* based on previous hypothesis with cave arachnids, specifically, those inhabiting the same cave system. For instance, members of the genus *Alacran*, which colonized the entire system in one single event about 65 Mya (VOLSCHENK & PRENDINI 2008; VIGNOLI & PRENDINI 2009), in a precursor cave before the formation of the Rio Petlapa (SANTIBAÑEZ-LÓPEZ et al. 2014). In addition, members of the tarantula genus *Hemirrhagus* Simon, 1903, which according with unpublished data, there are at least three different species in the
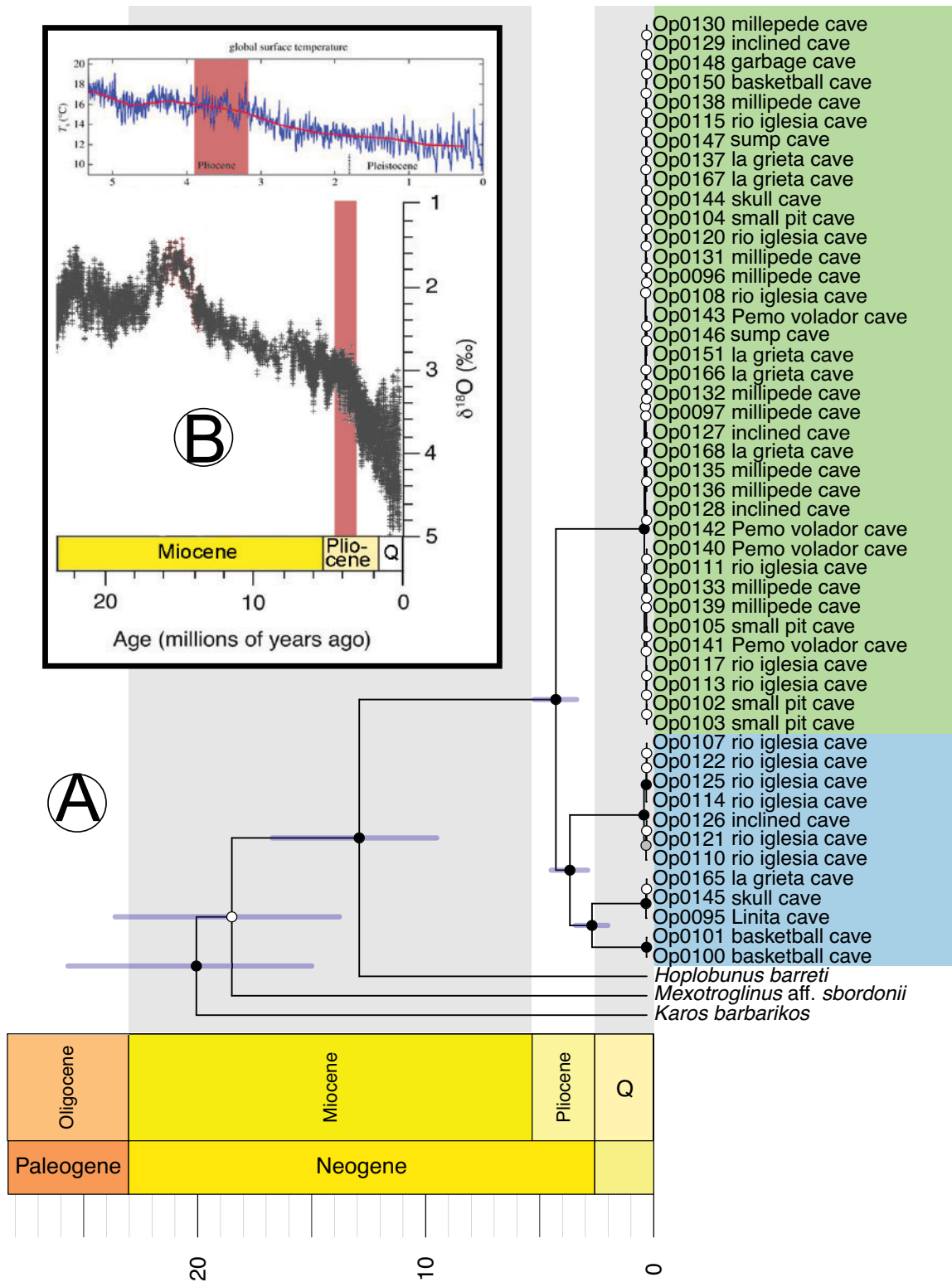
Fig. 12. Dated chronogram of the lineages of *Minisge* gen.n. (**A**) dated phylogeny obtained using BEAST under a strict clock. Lineages of *Minisge kanoni* sp.n. in blue, of *Minisge sagai* sp.n. in green. Dark circles are posterior probability values between 0.9 and 1.0, white circles with lower posterior probability values. (**B**) Inset graphics of the surface temperature during Miocene, Pliocene and Pleistocene periods, showing (in red) the increase of temperature about 3.5 and 4 Mya, taken and modified from Hansen et al. (2013) and Zachos et al. (2008).

Huautla Cave System, and they do not share a common ancestor, suggesting multiple invasions to the cave. Finally, species of undescribed opiliones *Huasteca* sp. and *Stygnopsis* sp., and the schizomid *Stenochrus magico* Monjaraz-Ruedas & Francke, 2018, which have a single species distributed in the entire cave system, much like *M. sagai*, suggest also one single relatively recent colonization event.

5. Conclusions

Caves are excellent evolutionary laboratories for biological studies. For the first time, an exceptional case of a troglomorphic harvestman lineage formed by two sister species has been recorded for the Huautla Cave System, one of the deepest cave systems in the world. Through barcoding, we were able to elucidate the evolutionary history of the two species inside the cave system. *M. sagai* inhabits shallower passages and exhibits a lesser degree in troglomorphic characters and a conserved genetic structure, showing a unique haplotype. In contrast, *M. kanoni* inhabits deeper passages, exhibiting a larger degree in troglomorphic characters, and is subdivided into three or four species under molecular-based delimitation methods with six different haplotypes and higher genetic distances between different populations. Further collections of specimens, and possibly the addition of data from more molecular markers could elucidate how this lineage colonized and diversified within the Huautla Cave System.

6. Acknowledgements

7. References

ACOSTA L., PÉREZ-GONZÁLEZ A., TOURINHO A.L. 2007. Methods for taxonomic study. Pp. 494–510 in: PINTO-DA-ROCHA R., MACHADO G., GIRIBET G. (eds), Harvestmen. The Biology of Opiliones. – Harvard University Press, Cambridge, Massachusetts. 597 pp.

BARR T.C., HOLSINGER J.R. 1985. Speciation in cave faunas. – Annual Review of Ecology and Systematics **16**: 313–337. doi: 10.1146/annurev.16.110185.001525.

BELL M.A., LLOYD G.T. 2015. Strap: an R package for plotting phylogenies against stratigraphy and assessing their stratigraphic congruence. – Palaeontology **58**: 379–389. doi:10.1111/pala.12142

BRYSON R.W., PRENDINI L., SAVARY W.E., PEARMAN P.B. 2014. Caves as microrefugia: Pleistocene phylogeography of the troglophilic North American scorpion *Pseudouroctonus reddelli*. – BMC Evolutionary Biology **14**: 9. doi:10.1186/1471-2148-14-9

CLEMENT M., POSADA D., CRANDALL K.A. 2000. TCS: A computer program to estimate gene genealogies. – Molecular Ecology **9**: 1657–1659. doi:10.1046/j.1365-294x.2000.01020.x

CRUZ-LÓPEZ J.A., FRANCKE O.F. 2015. Cladistic analysis and taxonomic revision of the genus *Karos* Goodnight & Goodnight, 1944 (Opiliones, Laniatores, Stygnopsidae). – Zoological Journal of the Linnean Society **175**: 827–891. doi:10.1111/zoj.12299

CRUZ-LÓPEZ J.A., FRANCKE O.F. 2017. Total evidence phylogeny of the North American harvestman family Stygnopsidae (Opiliones: Laniatores: Grassatores) reveals hidden diversity. – Invertebrate Systematics **31**: 317–360. doi:10.1071/IS16053

CRUZ-LÓPEZ J.A., PROUD D., PÉREZ-GONZÁLEZ A. 2016. When troglomorphism dupes taxonomists: morphology and molecules reveal the first pyramidopid harvestman (Arachnida, Opiliones, Pyramidopidae) from the New World. – Zoological Journal of the Linnean Society **177**: 602–620. doi:10.1111/zoj.12382

CULVER D.C. 2016. Karst environment. – Zeitschrift für Geomorphologie **60**: 103–117. doi:10.1127/zfg_suppl/2016/00306

CULVER D.C., KANE T.C., FONG D.W. 1995. Adaptations and Natural Selection in Caves: The Evolution of *Gammarus minus*. 1st edn. – Harvard University Press, Cambridge, Massachusetts. 223 pp.

DARRIBA D., TABOADA D.L., DOALLO R., POSADA D. 2012. jModelTest 2: more models, new heuristic and parallel computing. – Nature Methods **9**: 772. doi:10.1038/nmeth.2109

DERKARABETIAN S., STEINMANN D.B., HEDIN M. 2010. Repeated and time-correlated morphological convergence in cave-dwelling harvestmen (Opiliones, Laniatores) from Montane Western North America. – PLoS ONE **5**: e10388. doi:10.1371/journal.pone.0010388

DERKARABETIAN S., LEDFORD J., HEDIN M. 2011. Genetic diversification without obvious genitalic morphological divergence in harvestmen (Opiliones, Laniatores, *Sclerobunus robustus*) from montane sky islands of western North America. – Molecular Phylogenetics and Evolution **61**: 844–853. doi:10.1016/j.ympev.2011.08.004

DERKARABETIAN S., HEDIN M. 2014. Integrative taxonomy and species delimitation in harvestmen: A revision of the Western North American genus *Sclerobunus* (Opiliones: Laniatores: Travunioidea). – PLoS ONE **9**: e104982. doi:10.1371/journal.pone.0104982

DIDODEMICO A., HEDIN M. 2016. New species in the *Sitalcina sura* species group (Opiliones, Laniatores, Phalangodidae), with evidence for a biogeographical link between California desert canyons and Arizona sky islands. – ZooKeys **586**: 1–36. doi:10.3897/zookeys.586.7832

DRUMMOND A.J., SUCHARD M.A., XIE D., RAMBAUT A. 2012. Bayesian phylogenetics with BEAUti and the BEAST 1.7. – Molecular Biology and Evolution **29**: 1969–1973. doi:10.1093/molbev/mss075

EDGAR R.C. 2004. MUSCLE: multiple sequence alignment with high accuracy and high throughput. – Nucleic Acids Research. **32**: 1792–1797. doi:10.1093/nar/gkh340

EMATA K.N., HEDIN M. 2016. From the mountains to the coast and back again: Ancient biogeography in a radiation of short-range endemic harvestmen from California. – Molecular Phylogenetics and Evolution **98**: 233–243. doi:10.1016/j.ympev.2016.02.002

FERNÁNDEZ R., GIRIBET G. 2014. Phylogeography and species delimitation in the New Zealand endemic, genetically hypervariable harvestman species, *Aoraki denticulata* (Arachnida, Opiliones, Cyphophthalmi). – Invertebrate Systematics **28**: 401–414. doi:10.1071/IS14009

FOLMER O., BLACK M., HOEH W., LUTZ R. VRIJENHOEK R.C. 1994. DNA primers for amplification of mitochondrial cytochrome *c* oxidase subunit I from diverse metazoan invertebrates. – Molecular Marine Biology and Biotechnology **3**: 294–299.

GALAN C., HERRERA F. 1998. Fauna cavernícola. Ambiente y evolución. – Boletín de la Sociedad Venezolana de Espeleología **32**: 13–43.

HANSEN J., SATO M., RUSSELL G., KHARECHA P. 2013. Climate sensitivity sea level and atmospheric carbon dioxide. – Philosophical Transactions of the Royal Society **371**: e20120294. doi:10.1098/rsta.2012.0294.

HEBERT P.D.N., CYWINSKA A., BALL S.L., DEWAARD J.R. 2003. Biological identifications through DNA barcodes. – Proceedings Biological Sciences **270**: 313–321. doi:10.1098/rspb.2002.2218

HEBERT P.D.N., PENTON E.H., BURNS J.M., JANZEN D.H., HALLWACHS W. 2004. Ten species in one: DNA barcoding reveals cryptic species in the Neotropical skipper butterfly *Astraptes fulgerator*. – Proceedings of the National Academy of Sciences of the United States of America **101**: 14812–14817. doi:10.1073/pnas.0406166101

HEDIN M., THOMAS S.M. 2010. Molecular systematics of eastern North American Phalangodidae (Arachnida: Opiliones: Laniatores), demonstrating convergent morphological evolution in caves. – Molecular Phylogenetics and Evolution **54**: 107–121. doi:10.1016/j.ympev.2009.08.020

HEWITT G.M. 1996. Some genetic consequences of ice ages, and their role in divergence and speciation. – Biological Journal of the Linnean Society **58**: 247–276. doi:10.1111/j.1095-8312.1996.tb01434.x.

HOWARTH F.G., HOCH H. 2012. Adaptative shifts. Pp. 9–17 in: WHITE W.B., CULVER D.C. (eds), Encyclopedia of Caves. 2nd edn. – Tokyo, Academic Press. 966 pp.

HÜPPOP K. 2012. Adaptation to low food. Pp. 1–9 in: WHITE W.B., CULVER D.C. (eds), Encyclopedia of Caves. 2nd edn. – Tokyo, Academic Press. 966 pp.

JEFFERY W.R. 2005. Adaptive evolution of eye degeneration in the Mexican blind cavefish. – Journal of Heredity **96**: 185–196. doi:10.1093/jhered/esi028

JUAN C., GUZIK M.T., JAUME D., COOPER S.J.B. 2010. Evolution in caves: Darwin's wrecks of ancient life' in the molecular era. – Molecular Ecology **19**: 3865–3880. doi:10.1111/j.1365-294X.2010.04759.x.

KEARSE M., MOIR R., WILSON A., STONES-HAVAS S., CHEUNG M., STURROCK S., BUXTON S., COOPER S., MARKOWITZ S., DURAN C., THIERER T., ASHTON T., MENTJIES P., DRUMMOND A. 2012. Geneious basic: an integrated and expandable desktop software platform for the organization and analysis of sequence data. – Bioinformatics **28**: 1647–1649. doi:10.1093/bioinformatics/bts199

KUMAR S., STECHER G., TAMURA K. 2016. MEGA7: Molecular Evolutionary Genetics Analysis version 7.0 for bigger datasets. – Molecular Biology and Evolution **33**: 1870–1874. doi:10.1093/molbev/msw054

KURY A.B., VILLARREAL M.O. 2015. The prickly blade mapped: establishing homologies and a chaetotaxy for macrosetae of penis ventral plate in Gonyleptoidea (Arachnida, Opiliones, Laniatores). – Zoological Journal of the Linnean Society **174**: 1–46. doi:10.1111/zoj.12225

KURY A.B., MEDRANO M. 2016. Review of terminology for the outline of dorsal scutum in Laniatores (Arachnida, Opiliones). – Zootaxa **4097**: 130–134. doi:10.11646/zootaxa.4097.1.9

LANFEAR R., CALCOTT B., HO S.Y.M., GUINDON S. 2012. PartitionFinder: Combined selection of partitioning schemes and substitution models for phylogenetic analyses. – Molecular Biology and Evolution **29**: 1695–1701. doi:10.1093/molbev/mss020

LEIGH J.W., BRYANT D. 2015. Popart: Full-feature software for haplotype network construction. – Methods in Ecology and Evolution **6**: 1110–1116. doi:10.1111/2041-210X.12410

MADDEN T. 2003. The BLAST sequence analysis tool. In: MCENTYRE J., OSTELL J. (eds), The NBCI Handbook. 2nd edn. – Bethesda, National Center for Biotechnology Information, URL <www.ncbi.nlm.nih.gov/books/NBK153387/> [accessed 15 December 2017].

MADDISON W.P., MADDISON D.R. 2015. Mesquite: a modular system for evolutionary analysis. Ver. 3.2. – URL <http://mesquiteproject.org> [accessed 05 January 2018].

MILLER M.A., PFEIFFER W., SCHWARTZ T. 2010. Creating the CIPRES Science Gateway for inference of large phylogenetic trees. In: Proceedings of the Gateway Computing Environments Workshop (GCE). – New Orleans, 1–8.

PAPADOPOULOU A., ANASTASIOU I., VOGLER A.P. 2010. Revisiting the insect mitochondrial molecular clock: the mid-Aegean trench calibration. – Molecular Biology and Evolution **27**: 1659–1672. doi:10.1093/molbev/msq051.

PONS J., BARRACLOUGH T., GÓMEZ-ZURITA J., CARDOSO A., DURAN D., HAZELL S., KAMOUN S., SUMLIN W., VOGLER A. 2006. Sequence-based species delimitation for the DNA taxonomy of undescribed insects. – Systematic Biology **55**: 595–609. doi:10.1080/10635150600852011

PUILLANDRE N., LAMBERT A., BROUILLET S., ACHAZ G. 2012. ABGD, Automatic Barcode Gap Discovery for primary species delimitation. – Molecular Ecology **21**: 1864–1877. doi:10.1111/j.1365-294X.2011.05239.x

RAMBAUT A., SUCHARD M.A., XIE D., DRUMMOND A.J. 2014. TRACER v. 1.6. – URL <http://beast.bio.ed.ac.uk/Tracer> [accessed 01 December 2017].

REDDELL J.R. 2012. Spiders and related groups. Pp. 786–797 in: WHITE W.B., CULVER D.C. (eds), Encyclopedia of Caves. 2nd edn. – Tokyo, Academic Press. 966 pp.

RIBERA C. 2004. Arachnida. Pp. 146–154 in: GUNN J. (ed.), Encyclopedia of Caves and Karst Science 1st edn. – New York, Taylor & Francis. 1940 pp.

RONQUIST F., HUESENBECK J.P. 2003. MrBayes 3: Bayesian phylogenetic inference under mixed models. – Bioinformatics **19**: 1572–1574.

SANTIBÁÑEZ-LÓPEZ C.E., FRANCKE O.F., PRENDINI L. 2014. Shining a light into the world's deepest caves: phylogenetic systematics of the troglobitic scorpion genus *Alacran* Francke, 1982 (Typhlochactidae: Alacraninae). – Invertebrate Systematics **28**: 643–664. doi:10.1071/IS14035

SBORDONI V., ALLEGRUCCI C., CESARONI D. 2000. Population genetic structure, speciation and evolutionary rates in cave-dwelling organisms. Pp. 450–483 in: WILKENS H., CULVER D.C., HUMPHREYS W.F. (eds), Ecosystems of the World Chapter 24: Subterranean Ecosystems. – San Diego, Elsevier. 791 pp.

SCHÖNHOFER A.L., VERNESI C., MARTENS J., HEDIN M. 2015. Molecular phylogeny, biogeographic history, and evolution of cave-dwelling taxa in the European harvestman genus *Ischyropsalis* (Opiliones: Dyspnoi). – Journal of Arachnology **43**: 40–53. doi:10.1636/H14-39.1

SHARMA P.P., GIRIBET G. 2009. Sandokanid phylogeny based on eight molecular markers – The evolution of a Southeast Asian endemic family of Laniatores (Arachnida, Opiliones). – Molecular Phylogenetics and Evolution **52**: 432–447. doi:10.1016/j.ympev.2009.03.013

SHARMA P.P., GIRIBET G. 2011. The evolutionary and biogeographic history of the armoured harvestmen – Laniatores phylogeny based on ten molecular markers, with the description of two new families of Opiliones (Arachnida). – Invertebrate Systematics **25**: 106–142. doi:10.1071/IS11002

SIMON K.S. 2012. Cave ecosystems. Pp. 99–102 in: WHITE W.B., CULVER D.C. (eds), Encyclopedia of Caves. 2nd edn. – Tokyo, Academic Press. 966 pp.

STAMATAKIS A. 2014. RaxML version 8: a tool for phylogenetic analysis and post-analysis of large phylogenies. – Bioinformatics **30**: 1312–1313. doi:10.1093/bioinformatics/btu033

STEELE C.W., SMITH J.H. 2012. Sistema Huautla, Mexico. Pp. 712–718 in: WHITE W.B., CULVER D.C. (eds), Encyclopedia of Caves. 2nd edn. – Tokyo, Academic Press. 966 pp.

THOMAS S.M., HEDIN M. 2008. Multigenic phylogeographic divergence in the paleoendemic southern Appalachian opilionid *Fumontana deprehendor* Shear (Opiliones, Laniatores, Triaenonychidae). – Molecular Phylogenetics and Evolution **46**: 645–658. doi:10.1016/j.ympev.2007.10.013

TRAJANO E., COBOLLI M. 2012. Evolution of lineages. Pp. 295–304 in: WHITE W.B., CULVER D.C. (eds), Encyclopedia of Caves. 2nd edn. – Tokyo, Academic Press. 966 pp.

Vɪɢɴᴏʟɪ V., Pʀᴇɴᴅɪɴɪ L. 2009. Systematic revision of the troglomorphic North American scorpion family Typhlochactidae (Scorpiones, Chactoidea). – Bulletin of the American Museum of Natural History **326**.

Vᴏʟsᴄʜᴇɴᴋ E., Pʀᴇɴᴅɪɴɪ L. 2008. *Aops oncodactylus*, gen. et sp. nov., the first troglobitic urodacid (Urodacidae: Scorpiones), with a re-assessment of cavernicolous, troglobitic and troglomorphic scorpions. – Invertebrate Systematics **22**: 235–257. doi:10.1071/IS06054

Wɪᴇɴs J.J., Gʀᴀʜᴀᴍ C.H. 2005. Niche conservatism: integrating evolution, ecology and conservation biology. – Annual Review of Ecology, Evolution, and Systematics **36**: 519–539. doi:10.1146/annurev.ecolsys.36.102803.095431

Zᴀᴄʜᴏs J.C., Dɪᴄᴋᴇɴs G.R., Zᴇᴇʙᴇ R.E. 2008. An early Cenozoic perspective on greenhouse warming and carbon-cycle dynamics. – Nature **451**: 279–283. doi:10.1038/nature06588.

Zʜᴀɴɢ J., Kᴀᴘʟɪ P., Pᴀᴠʟɪᴅɪs P., Sᴛᴀᴍᴀᴛᴀᴋɪs A. 2013. A general species delimitation method with applications to phylogenetic placements. – Bioinformatics **29**: 2869–2876. doi:10.1093/bioinformatics/btt499

Electronic Supplement Files

at http://www.senckenberg.de/arthropod-systematics

File 1: cruzlopez&al-opilionesstygnopsidae-asp2019-electronic supplement-1.xls — Genbank accession numbers of the CO1 sequences generated in the present study. — DOI: 10.26049/ASP77-2-2019-06/1

File 2: cruzlopez&al-opilionesstygnopsidae-asp2019-electronic supplement-2.nex — Data matrix of CO1 sequences for Maximum Likelihood analysis. — DOI: 10.26049/ASP77-2-2019-06/2

File 3: cruzlopez&al-opilionesstygnopsidae-asp2019-electronic supplement-3.nex — Data matrix of CO1 sequences for Bayesian Inference analysis. — DOI: 10.26049/ASP77-2-2019-06/3

File 4: cruzlopez&al-opilionesstygnopsidae-asp2019-electronic supplement-4.tre — Dated tree obtained from BEAST analysis. — DOI: 10.26049/ASP77-2-2019-06/4

File 5: cruzlopez&al-opilionesstygnopsidae-asp2019-electronic supplement-5.xls — Matrix of uncorrected genetic distances among *Minisge* populations. — DOI: 10.26049/ASP77-2-2019-06/5

File 6: cruzlopez&al-opilionesstygnopsidae-asp2019-electronic supplement-6.nex — Data matrix of CO1 sequences used in PopArt for haplotype network. — DOI: 10.26049/ASP77-2-2019-06/6

File 7: cruzlopez&al-opilionesstygnopsidae-asp2019-electronic supplement-7.txt — Results of the ABGD species delimitation analysis. — DOI: 10.26049/ASP77-2-2019-06/7

File 8: cruzlopez&al-opilionesstygnopsidae-asp2019-electronic supplement-8.tree — Results of the GMYC species delimitation analysis. — DOI: 10.26049/ASP77-2-2019-06/8

File 9: cruzlopez&al-opilionesstygnopsidae-asp2019-electronic supplement-9.tree — Results of the bPTP species delimitation analysis. — DOI: 10.26049/ASP77-2-2019-06/9

Zoobank Registrations

at http://zoobank.org

Present article: http://zoobank.org/urn:lsid:zoobank.org:pub:860108A9-0542-4E50-8483-3712A4A1DC01

***Minisge* Cruz-López, Monjaraz-Ruedas & Francke, 2019:** http://zoobank.org/urn:lsid:zoobank.org:act:D21FB7C2-185E-4832-BD54-B05124B3D8AC

***Minisge sagai* Cruz-López, Monjaraz-Ruedas & Francke, 2019:** http://zoobank.org/urn:lsid:zoobank.org:act:9C1DC9CD-39B8-4422-A210-26113F637E18

***Minisge kanoni* Cruz-López, Monjaraz-Ruedas & Francke, 2019:** http://zoobank.org/urn:lsid:zoobank.org:act:05177696-DED8-4725-A54B-CED1C8FDD14B

Authors' Contributions

RMR has done molecular work. JACL and RMR have done all analyses. JACL has done the taxonomic work. JACL, RMR and OFF collected the specimens and have written the manuscript.